Friction **9**(5): 1138–1149 (2021)
https://doi.org/10.1007/s40544-020-0411-2
ISSN 2223-7690
CN 10-1237/TH
RESEARCH ARTICLE

Quantitative analysis of the tribological properties of phosphate glass at the nano- and macro-scales

Huimin QI[1], **Wen HU**[1], **Hongtu HE**[1], **Yafeng ZHANG**[1], **Chenfei SONG**[2], **Jiaxin YU**[1,2,*]

[1] *Key Laboratory of Testing Technology for Manufacturing Process in Ministry of Education, State Key Laboratory of Environment-friendly Energy Materials, Southwest University of Science and Technology, Mianyang 621010, China*

[2] *National United Engineering Laboratory for Advanced Bearing Tribology, Henan University of Science and Technology, Luoyang 471023, China*

Received: 11 October 2019 / Revised: 06 January 2020 / Accepted: 09 May 2020

Abstract: Processing (grinding, polishing) of phosphate laser (PL) glass involves material removal at two vastly different (spatial) scales. In this study, the nano- and macro-tribological properties of PL glass are investigated by rubbing the glass against a SiO_2 counter-surface in both dry and humid conditions. The results indicate that the friction of the PL glass/SiO_2 pair has opposing trends at the nano- and macro-scales. At the nanoscale, the friction coefficient (COF) in humid air is much higher than in dry air, which is attributed to the capillary effect of the absorbed water-film at the interface. At the macroscale, on the other hand, the COF in humid air is lower than in dry air, because the water-related mechanochemical wear makes the worn surface less susceptible to cracking. Material removal for PL glass is better facilitated by humid air than by dry air at both scales, because the stress-enhanced hydrolysis accelerates the material-removal process in glass. Moreover, the material-removal is more sensitive to contact pressure at the macroscale, because stronger mechanical-interaction occurs during material removal at the macroscale with the multi asperity contact mode. At the macroscale, the material removal is more sensitive to contact pressure in humid air compared to dry air. Because almost all mechanical energy is used to remove material in humid air, and most of the mechanical energy is used to produce cracks in PL glass in dry air. The results of this study can help optimize the multi-scale surface processing of optical glasses.

Keywords: phosphate glass; friction; wear; water; hydrolysis; tribochemistry

1 Introduction

Nd-doped phosphate laser (PL) glasses are an ideal gain medium for high peak-power solid-state lasers because of their high optical energy-storage capacity. For this reason, they are widely used for power amplification in high peak-power laser-systems [1, 2]. To provide a high-quality optical surface, PL glasses need to be processed via grinding to ensure high surface precision. This process involves material removal at the macroscale [3]. Subsequently, the PL glasses are polished to provide an ultra-smooth and defect-free surface, which involves material removal at the nanoscale [4]. In both processes, the material removal occurs due to tribological interaction between the grinding/ polishing particles and the glass substrate. In other words, understanding the tribological properties of PL glass at both nano- and macro-scales is critical.

Owing to varying contact areas and shear stresses,

* Corresponding author: Jiaxin YU, E-mail: yujiaxin@swust.edu.cn

the tribological properties of many materials, such as metals, semiconductors, and ceramics, are often significantly different between the nanoscale and macroscale [5–13]. For metals, Kumar and Bhushan [8] found that nitriding reveals the different nano- and macro-tribological properties of H-13 steel. At the nanoscale, the COFs of pristine H-13 steel and nitride H-13 steel were found to be almost equal. However, the wear depth of nitride H-13 steel was lower than that for the pristine sample as nitriding improved the nanohardness of H-13 steel. However, the COF of nitride H-13 steel at the macroscale was found to be lower than that for the pristine H-13 steel, although the wear depth of nitride H-13 steel was higher than that of the pristine sample owing to increased material exfoliation. For semiconductors, Yu et al. [9, 10, 14–16] found that the surface hydrophilicity exhibited a critical effect on the nano-tribological properties of Si(100): The interfacial water-film increased both the capillary force and friction force, as well as water-related tribo-chemical wear. However, the surface hydrophilicity hardly affected the macro-tribological performance of Si(100) because asperities can easily penetrate the interfacial water-film owing to the very high local contact-pressure due to the multiasperity contact [11]. For ceramic materials, Zum et al. [12] showed that a humid environment hardly affects the COF of SiC ceramics at the nanoscale. However, with increasing humidity, the COF increased but the wear rate decreased at the macroscale, because the wear mechanism changed from mechanical to tribo-chemical wear. Despite all these studies, a quantitatively comparative analysis of the nano- and macro-tribological properties of glasses has not been performed.

Because oxide glasses are typically brittle materials, the friction-induced fracture is expected to be a major damage mode with regard to wear at the macroscale [17, 18]. However, at the nanoscale, the brittle glasses may also suffer from ductile material removal when the contact pressure is lower than the fracture strength [19, 20]. In addition, the tribological properties of glasses at both the nanoscale and the macroscale depend not only on the mechanical properties of the materials themselves but also on the environment [21, 22]. Water molecules are an important environmental factor that could affect the tribological properties of glasses [23]. Owing to the presence of water molecules, the hydrolysis, ion exchange, and surface hydration of the glass network easily occur, which contributes to the friction and wear performance of most oxide glasses [24–26]. As there is no cross-linked backbone structure, phosphate glasses usually show much poorer water-resistance than most silicate glasses [27]. As a result, water molecules can attack a glass network more easily under the assistance of frictional shear stress. Our previous study also revealed that, with the help of water molecules, material removal rates are higher, and cracking of PL glass occurs more easily than BK7 silicate glass in liquid water [17]. Due to the different contact modes at different scales (single-asperity contact for nanowear, multiasperity contact for macrowear), the contact stress can vary with respect to nano- and macro-tribological properties. This can further affect not only the damage mode of glass directly but also the degree of water-related tribo-chemical wear. However, the exact difference between the nano- and macro-tribological properties of PL glass with or without the participation of water molecules remains unclear.

In this study, the nano- and macro-tribological properties of a PL glass were investigated using an atomic force microscope and a universal reciprocating sliding tribometer, respectively. The experiments were operated in both dry and humid air. The COF and material removal volumes were quantitatively evaluated for all conditions. The damage modes were also analyzed at both scales. The differences in friction and wear between nanoscale and macroscale were ascertained, and the role of contact stress, with regard to glass deformation and mechanochemical wear, was investigated. The results provide new insights into the tribological properties of glasses in relation to surface processing.

2 Materials and methods

2.1 Materials

Polished N31 Nd-doped PL glass slides (5 wt%–

60 wt% P_2O_5, 8 wt%–12 wt% Al_2O_3, 10 wt%–14 wt% K_2O, 8 wt%–12 wt% BaO, 2 wt%–3 wt% Li_2O, 1 wt%–3 wt% Nd_2O_3), with the dimensions of 20 mm × 20 mm × 2 mm provided by Shanghai Daheng Optics and Fine Mechanics Co., Ltd., China, were used as glass substrates. Before the tribology tests, all the glass samples were stored in an electronic moisture-proof box, where the relative humidity was set below 10% and the temperature was maintained at room temperature. Using an atomic force microscope (AFM, SPI3800N, Seiko, Japan), the root-mean-square (RMS) roughness of the glass was measured as 0.57 nm for an area of 3 μm × 3 μm. The elastic modulus and the nanohardness of the PL glass were measured as 66.6 and 6.0 GPa, respectively, using a nano-indenter (G200, Keysight, USA). Using a contact-angle tester (DSA30E, KRUSS, Germany), the water contact-angle of the glass substrate was determined as 29.1° in humid air (for a humidity level of 55%). Before every tribological test, the glass slides were washed with ethanol and pure water for 5 min using an ultrasonic cleaning machine. They were then blow-dried using high-purity nitrogen.

2.2 Nanoscale tribological tests

As shown in Fig. 1(a), all nanoscale friction and wear tests were performed using an AFM equipped with an environmental chamber. The frictional counter-surface was fused silica (SiO_2) microsphere, which is a typical polishing particle used in glass surface processing. It was glued to the end of the AFM probe cantilever (Novascan Technologies, Ames, IA; the inset in Fig. 1(a)). The radius of the silica microsphere was ~1 μm. The friction mode in the test was linear reciprocating sliding friction. The applied load varied from 3 to 5 μN. The sliding displacement and the sliding velocity were set to 2 μm and 8 μm/s, respectively. The number of sliding cycles was 100. The temperature for the test was maintained at 20–22 ℃. All the tests were performed in dry air at a relative humidity below 2% and humid air at a relative humidity of 50%–60%. After the tests, the topography of the wear area on the PL glass surface was scanned using the tapping mode with a sensitive silicon-nitride tip with a curvature radius of 10 nm (Nanosensors, Switzerland). Before all the tribological tests, the spring constant of the AFM probe was calibrated using a calibration probe with a force constant of 3.438 N/m (CLFC-NOBO, Bruker, USA). After calibration, the spring constant was found to be 41.5 N/m. Then, the friction force was calibrated using a modified wedge method with a silicon grating and a wedge angle of 54°44' (TGF11, MikroMasch, Estonia) [28]. The adhesion forces (pull-off forces) between the PL glass and the silica microsphere were measured to be 0.5 and 1.2 μN in dry and humid air, respectively.

2.3 Macroscale tribological tests

As shown in Fig. 1(b), all the macroscale friction and wear tests were performed using a universal ball-on-flat tribometer (MFT-3000, Rtec, USA), which was equipped with a home-made environment chamber. The friction mode used in the test was also linear reciprocating sliding friction. Similar to the nanoscale test, the frictional counter-surface during the macroscale test was a fused silica ball with a radius of 2 mm. The normal load during the test varied from 0.2 to 0.8 N, the sliding displacement

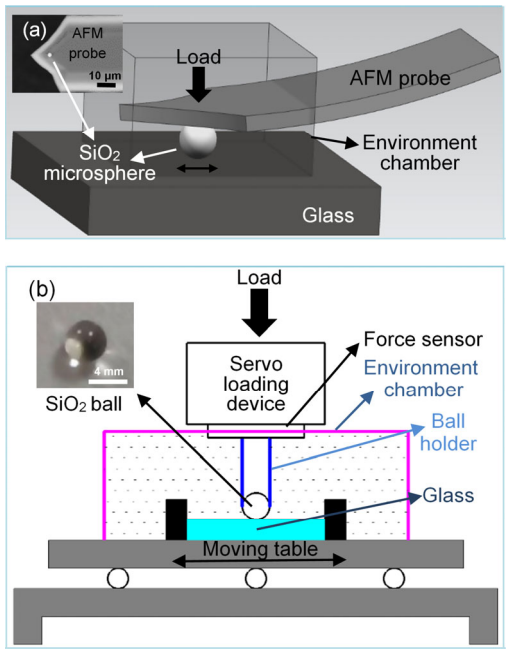

Fig. 1 Schematic of the tribological tests conducted at (a) the nanoscale using an atomic force microscope and (b) the macroscale using a universal ball-on-flat tribometer.

was 2 mm, and the sliding time was 68 min (the number of sliding cycles was 50). To equalize the effect of sliding velocity on the tribological property for both the nano- and macro-scales, the sliding velocity was set to 50 μm/s, which is similar to the sliding velocity of the nanoscale test. Similarly, all macroscale tests were performed at room temperature in dry air at a relative humidity below 2% and humid air at a relative humidity of 50%–60%. After each experiment, the wear track in the PL glass was analyzed using a white light scanning profilometer (Rtec, USA). All the wear tracks were also investigated with an optical microscope (BX51-P, Olympus, Japan) to better understand the damage mode. The detailed experimental parameters for both the nano- and macro-scales are summarized in Table 1.

3 Results and discussion

3.1 Comparison of friction of PL glass with a SiO_2 counter-surface at the nano- and macro-scales

Figure 2(a) shows the nanoscale COF of a PL glass/SiO_2 pair as a function of the applied load after 100 sliding cycles, where the inset shows the measured friction-force for different loads under both dry and humid conditions. The COF was calculated as the ratio of the friction force to the sum of the applied load and adhesion force. In dry air, the COFs decreased slightly, during a load increase from 3 to 5 μN, and all the values almost keep around 0.04. The friction force only increased from 0.16 to 0.19 μN with increasing load. However, in humid air, both the COF and friction forces were much higher than in dry air. Furthermore, an increase in load from 3 to 5 μN resulted in an increase in the friction force from 2.0 to 2.6 μN, whereas the COF decreased from 0.48 to 0.42. The average COF in humid air was nine times higher than in dry air.

At the nanoscale, the friction force is the sum of interfacial friction and ploughing friction [29, 30]. Interfacial friction is the sum of the solid–solid interaction and the capillary effect. Ploughing friction, on the other hand, is determined by the ploughing plastic-deformation [31]. The specific friction mode greatly depends on the contact pressure between the friction pairs. Using the Hertz contact mode, the maximum contact pressure, P, between a sphere and flat can be calculated using Eq. (1) [32]:

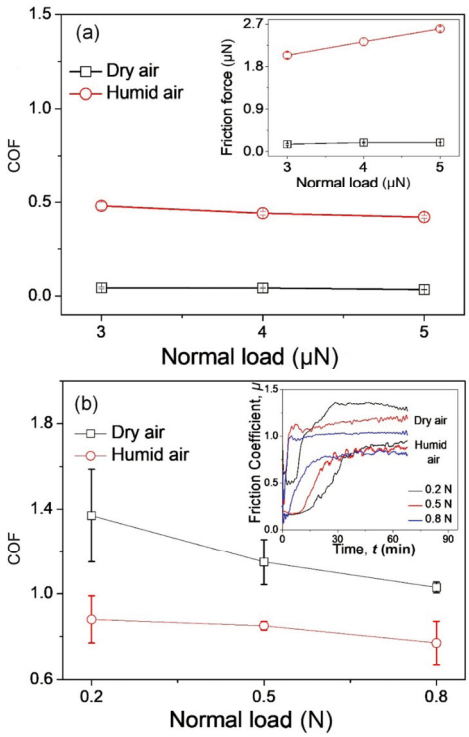

Fig. 2 COF of a PL glass/SiO_2 pair as a function of applied load at (a) the nanoscale and (b) the macroscale. The inset in (a) shows the measured friction force for different loads in dry and humid conditions, and the inset in (b) shows the measured real-time COF as a function of sliding time for different loads in the two environments.

Table 1 Details of the tribological test parameters at the nano- and macro-scales.

Equipment	Provider	Load range (N)	Counter-body radius (m)	Velocity (m/s)	Sliding cycles	Counter-body material
AFM	Seiko, Japan	10^{-6}	1×10^{-6}	8×10^{-6}	100	SiO_2 glass
Tribometer	Rtec, USA	10^{0}	2×10^{-3}	50×10^{-6}	50	SiO_2 glass

$$P = \left(\frac{6LE^{*2}}{\pi^3 R^2} \right)^{1/3} \quad (1)$$

where L is the normal load, E^* is the reduced elastic modulus of the sphere and flat materials, and R is the radius of the sphere. To determine the critical load when plastic deformation occurs in PL glass, different loads were used in nanoindentation tests that used a nano-indenter with a sphere diamond tip with a radius of 0.59 μm (Fig. S1, Electronic Supplementary Material (ESM)). When the normal load of 0.5 mN was applied, the loading and unloading curves did not coincide with each other, which indicated that plastic deformation had occurred. As a result, using Eq. (1), the maximum contact pressure for plastic deformation in PL glass was determined as 10.8 GPa. For the nanoscale friction test, the normal load was taken as the sum of the applied load and the adhesion force. As a result, the maximum normal load was 5.5 μN in dry air and 6.2 μN in the humid air. Using Eq. (1), the maximum contact stress during the nanoscale friction experiments was calculated as 1.12 GPa for dry air, and 1.17 GPa in humid air, which was only ~10% of the contact stress of the plastic deformation. Because of the low contact-pressure, there was no plastic ploughing for the nanoscale friction of the PL glass/SiO_2 pair. Thus, ploughing friction should not be considered in the nanoscale friction test for both dry and humid conditions.

As a result, interfacial friction dominates the friction mechanism of the PL glass/SiO_2 pair at the nanoscale in both dry and humid environments. The interfacial friction force, F_{int}, is defined as the shear force in the elastic contact region. Hence, F_{int} can be defined using Eq. (2):

$$F_{int} = S \times A_{int} \quad (2)$$

where S is the so-called shear stress, and A_{int} is the contact area between the SiO_2 microsphere and PL glass surface. The Hertz contact equation relates the contact radius for a known tip and a sample under a certain load [32]:

$$A_{int} = \pi \left(\frac{3RL}{4E^*} \right)^{2/3} \quad (3)$$

Using Eqs. (2) and (3), the interfacial COF, μ_{int}, can be expressed as

$$\mu_{int} = F_{int} / L = \pi S \left(\frac{3R}{4E^*} \right)^{2/3} L^{-1/3} \quad (4)$$

Equation (4) shows that the interfacial COF correlates negatively with the normal load. This is the reason why the COF of the PL glass/SiO_2 pair decreases with an increase in load under both dry and humid air conditions. Equation (4) also shows that the interfacial COF has a positive correlation with shear stress. In dry air, owing to the absence of water molecules, the capillary effect between the SiO_2 microsphere and PL glass can be neglected, and interfacial friction is mainly due to solid–solid interactions. As a result, the shear stress is determined by the van der Waals forces and the chemical bond force in dry conditions. In humid air, on the other hand, the PL surface is relatively hydrophilic. Based on the water contact-angle of PL glass and the relative humidity, the thickness of the water film at the PL glass/SiO_2 interface was calculated as 1.44 nm using the theory proposed by Xiao and Qian [33]. The interfacial water film increases the capillary effect, which, in turn, increases the shear stress between the PL glass/SiO_2 pair. Therefore, the COF is much higher in humid air than in dry air.

The friction of the PL glass/SiO_2 pair at the macroscale is different from at the nanoscale. Figure 2(b) shows the stable COF of PL glass/SiO_2 pair at the macroscale as a function of the normal load during 50 friction cycles. The inset in Fig. 2(b) shows the measured real-time COF as a function of sliding time for different loads under both dry and humid conditions. In dry air, the COF decreases from 1.37 to 1.03 as the load increases from 0.2 to 0.8 N. In humid air, however, the COF varies over a very limited range (0.77–0.88). The COF in dry air is significantly higher than that in humid air, which is the opposite of the nanoscale.

At the macroscale, the maximum Hertz contact stress was calculated as 0.23–0.37 GPa using Eq. (1), which is much lower than that for the nanoscale. However, the contact at the macroscale, between the PL glass and SiO_2 ball is a multiasperity contact. The roughness of the SiO_2 ball was measured

as ~20 nm for the contact region. If we assume that the asperity radius of the SiO_2 ball is 2 μm (much larger than the roughness), the Hertz contact pressure is as high as ~23 GPa for a load of 0.2 N, which is much higher than the contact pressure that occurs during plastic deformation (10.8 GPa). As a result, unlike the friction at the nanoscale, the friction of the PL glass/SiO_2 pair would be dominated by ploughing friction between contact asperities. Thus, the COF at the macroscale is much higher than that at the nanoscale. In dry air, typical dry ploughing friction occurs. The scratching and cracking, which are caused by multiasperity, make the wear track surface bumpy (Section 3.2), which results in a related high COF. In humid air, the water film at the PL glass/SiO_2 interface was very thin (1.44 nm). Because of the multi asperity contact, the contact stress at each asperity is high enough, and the asperity can penetrate the water film and the glass substrate. Therefore, the role capillary effect is weakened, and as a result, the friction force does not increase at the macroscale. On the contrary, the COF in humid air is lower than that in dry air because the water-related mechanochemical reaction makes material removal easier than in dry air, where the wear track surface would become smoother with less cracking. The mechanochemical wear that occurs in humid air is discussed in detail in the next section.

Figure 3 summarizes the COF for PL glass/SiO_2 pair as a function of the maximum Hertz contact stress for both scales. The friction of the PL glass/SiO_2 pair shows completely different trends for the two scales. At the nanoscale, owing to the single-asperity contact, the contact pressure is equal to the real contact pressure. The contact pressure is in the range of 0.86–1.16 GPa, which is lower than the stress under which plastic deformation occurs. As a result, the interfacial friction dominates the friction process, and the COF is relatively low in both dry and humid air. The higher COF in humid air is attributed to the capillary effect due to the interfacial absorbed water-film. At the macroscale, owing to the multiasperity contact, the contact-stress is only in the range of 0.23–0.37 GPa. However, the real contact stress is expected to be much higher than the contact-stress. The friction at each asperity is dominated by ploughing friction, which causes relatively high COFs at the macroscale compared to the nanoscale for both dry and humid air. The lower COF in humid air occurs because water-related mechanochemical wear makes the wear track surface smoother.

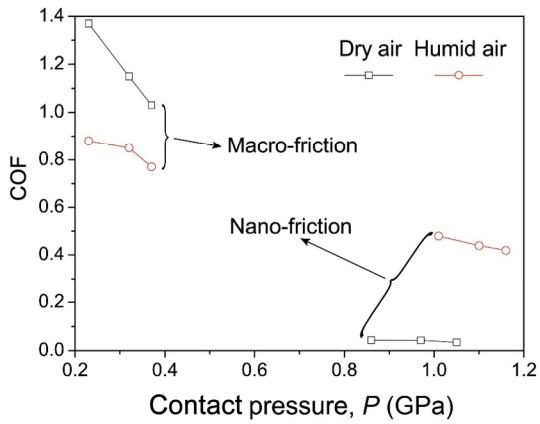

Fig. 3 COF of the PL glass/SiO_2 pair as a function of the maximum Hertz contact stress at the nanoscale and macroscale.

3.2 Comparison of the wear properties of PL glass rubbed against a SiO_2 counter-surface at the nano- and macro-scales

To characterize the wear of PL glass quantitatively, AFM images and optical profilometry images of wear tracks were obtained for both the nanoscale and the macroscale, respectively. Figure 4(a) shows the AFM images of the nanoscale wear tracks on PL glass in both dry and humid air. After 100 cycles reciprocating friction in dry air, no visible friction-tracks were found on the glass surface even when the applied load was increased to a maximum of 5 μN. In contrast, visible grooves were found on the glass surface for all the load conditions. Some wear debris was also found at the sides of the wear track, which indicates that nanoscale material-removal took place. Figure 4(b) shows the wear volume for PL glass as a function of applied load in dry and humid air, which was estimated based on the cross-sectional profile lines of the wear tracks shown in the inset of Fig. 4(b). In dry air, the wear volume remained constant, at 0 nm^3, for all load conditions. However, in humid air, as the load increased from 3 to 5 μN, the wear volume increased sharply from

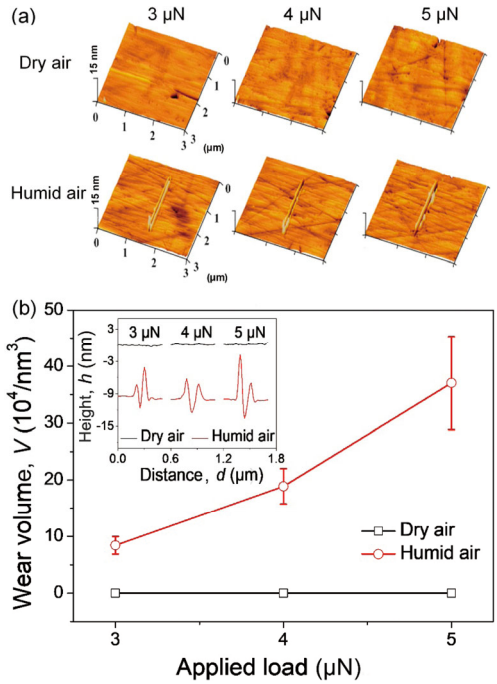

Fig. 4 (a) AFM topography images of the wear tracks for PL glass at the nanoscale in dry and humid air under different loads. (b) The wear volume of PL glass as a function of applied load in both dry and humid air, where the wear volume was estimated from the cross-sectional profile lines of the wear track shown in the inset.

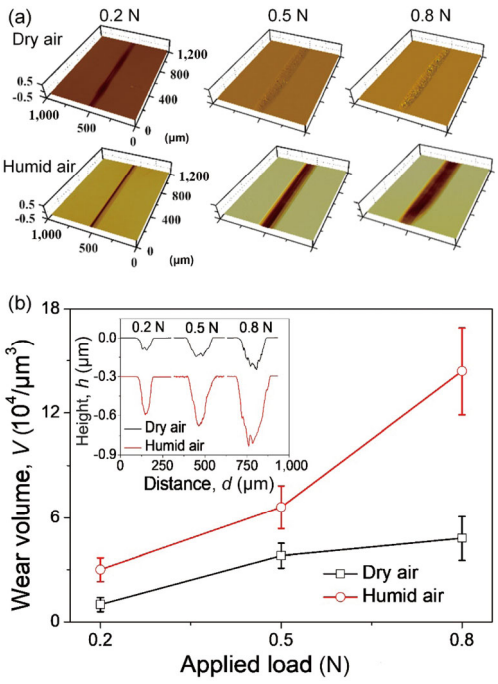

Fig. 5 (a) Optical profilometry images of the wear tracks of PL glass at the macroscale in dry and humid air under different loads. (b) The wear volume of PL glass as a function of applied load in both dry and humid air, where the wear volume was estimated from the cross-sectional profile lines of the wear track shown in the inset.

8.4×10^4 to 37.1×10^4 nm^3. These results revealed that the wear of PL glass was much more severe in humid air than in dry air at the nanoscale.

Figure 5(a) shows the optical profilometry images of macroscale wear-tracks on PL glass for both dry and humid air. Some obvious wear-grooves were observed on the glass surface in both the two environments. In dry air, the surface of the wear-grooves looked bumpy, but it seemed to be smoother in the humid air. According to the cross-sectional profile lines of these wear groove, Fig. 5(b) shows the wear volume of PL glass as a function of the applied load in dry and humid air at the macroscale. Although the wear volume of PL glass increased with increasing load for both environments, the increase ratio was higher in the humid air. Upon increasing the load from 0.2 to 0.8 N, the wear volume increased from 1.0×10^4 to 4.8×10^4 μm^3 in dry air, and from 3.0×10^4 to 14.4×10^4 μm^3 in the humid air, respectively. Furthermore, the wear volume of PL glass in humid air was larger than in dry air at the macroscale, which is similar to the trend observed at the nanoscale. It is plausible that the high wear of PL glass in humid air could share a similar mechanism at both scales.

The higher wear volume of PL glass at both scales in humid air indicates that the water molecules play an important role in accelerated material removal. The chemical reaction between water and oxide glass includes hydration, leaching, and hydrolysis [26]. The reaction degree is determined by the chemical stability of the glass network as well as external energy (such as mechanical and thermal). Comparing common silicate glasses, the chemical stability of phosphate glasses is low due to the lack of backbone cross-linking. Therefore, phosphate glasses can be attacked by water molecules relatively easy [27]. Although the reaction between water molecules and phosphate glass is very weak at room temperature (about 25 ℃), it can be enhanced by increasing the temperature [26]. In addition, at room temperature (about 25 ℃), the reaction between water molecules and phosphate glass can be intensified

in the presence of tensile stress and frictional shear-stress. Here, the reaction process can be regarded as stress-corrosion [22] and tribo-corrosion [34]. Stress enhanced hydrolysis and leaching are considered the main mechanisms, which can be described using Reactions (5) and (6), where M represents the metal ion in the glass network:

$$P–O–P + H_2O = P–OH + OH–P \quad (5)$$

$$P–O–M + H_2O = P–OM + OH–P \quad (6)$$

At the nanoscale, the contact between PL glass and the SiO_2 microsphere is elastic, and the shear stress is sufficiently low. As a result, reciprocating friction cannot produce any damage on the PL surface in dry air. In humid air, however, owing to the capillary effect, the frictional shear stress increases due to the much higher COF. The absorbed water molecules can react with the PL glass network under the high shear-stress, according to Reactions (5) and (6), which aids in the material removal from the glass substrate to generate visible wear grooves on the glass surface. The details of the nanowear of PL glass were described in our previous study [26]. At the macroscale, the increased wear volume in PL glass can also be explained by stress-enhanced hydrolysis or leaching. To verify this hypothesis, Raman spectra of wear debris on the PL glass surface under a load of 0.8 N in dry and humid air were recorded (Fig. 6). There is a clear peak at ~3,200 cm^{-1} for humid air, but nothing discernible for the dry air sample and the pristine surface without wear. In PL glass, the peaks appear from 2,950 to 3,450 cm^{-1}, which are typical for OH stretching [35, 36]. Therefore, the stronger peak at ~3,200 cm^{-1} in humid air indicates that more OH clusters were found in wear debris after wear in humid air compared to dry air. This implies that hydrolysis of the P–O–P network, or leaching of P–O–M bond, occurs during wear in PL glass in humid air (Reactions (5) and (6)), which confirms a water-related mechanochemical reaction in the humid air. This suggests that the increased wear volumes of PL glass in humid air at both scales share the same mechanochemical reaction mechanism.

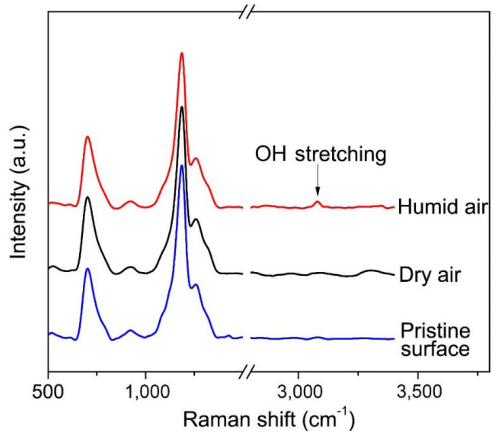

Fig. 6 Raman spectra of the wear debris attached to the wear track in PL glass after the glass is rubbed in the dry and humid air. For comparison, the Raman spectrum of a pristine glass surface without wear is also shown.

On the other hand, stress-enhanced hydrolysis also acts on the counter-body of the SiO_2 glass. Figure 7 shows photographs of the SiO_2 glass ball after rubbing in the dry and humid air. Larger wear-scars can be observed on the SiO_2 glass ball surface in humid air, which suggests that the water molecules also promote material removal of SiO_2 glass. This can also be explained by the stress-enhanced hydrolysis. Similar phenomena were also found in another borosilicate- and barium-boroaluminosilicate-glasses [24, 25], which indicates that, for many oxide glasses, frictional stress-enhanced hydrolysis is the typical mechanism through which water molecules facilitate material removal.

Figure 8 shows the wear volume growth-rate of PL glass, β, as a function of the maximum, P, for PL glass/SiO_2 pair, for both the nanoscale and the macroscale. Using the wear volume at the lowest load as a reference, the β at the higher load

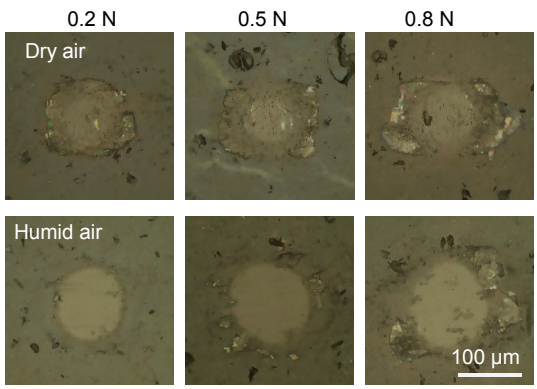

Fig. 7 Optical images of the wear scars on SiO_2 glass ball after rubbing in dry and humid air at the macroscale.

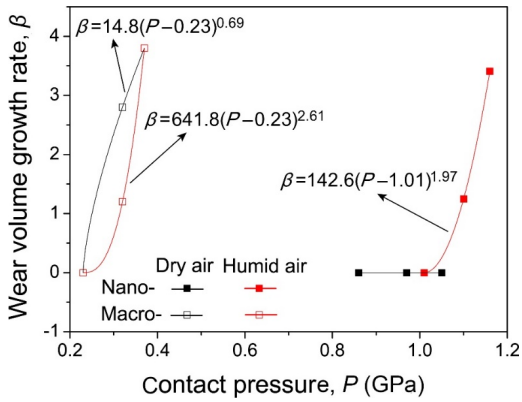

Fig. 8 β of PL glass as a function of the maximum Hertz contact stress at the nano- and macro-scale, where the plots were fitted by the power function.

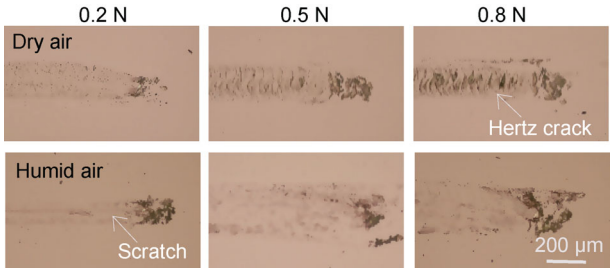

Fig. 9 Optical images of the wear tracks in PL glass after rubbing in dry and humid air at the macroscale.

can be calculated using $\beta = (V_i - V_0) / V_0$, where V_0 is the wear volume for the lowest load, and V_i is the wear volume for the other higher load, for each environment and each scale. For further quantitative analysis, the relationship between β and P was fitted using a power function:

$$\beta = a(P+b)P^m \tag{7}$$

where a, b, and m are the fit parameters. Furthermore, m can be defined as a pressure-sensitivity-exponent, and material removal occurs more easily when m is high. Due to no wear at the nanoscale in dry air, β can be considered 0 for all loads. For other experimental conditions, the fitting equations are shown in Fig. 8.

It can be found that m at the macroscale is 0.69 in dry air and 2.61 in the humid air. Material removal is more sensitive to contact pressure in humid air than dry air. This can be explained by the different damage modes in PL glass for dry and humid air. Figure 9 shows photographs of the wear tracks of PL glass after rubbing in the dry and humid air. In dry air, with increasing load, more Hertz cracks can be observed on the glass surface. This indicates cracking is an important damage mode, in addition to material removal. However, almost no cracking can be found in the wear tracks in the humid air. Furthermore, scratches, combined with a considerable quantity of wear debris, were observed in the wear track region, where material removal was the main damage mode due to the mechanochemical wear (stress-enhanced hydrolysis) in the humid air. That more mechanical energy is used to produce cracks in PL glass in dry air suggests a weaker material removal capability on the PL glass surface. In other words, material removal is less sensitive to contact pressure in dry air than in humid air.

In humid air, m is 1.97 at the nanoscale, which is lower than the 2.61 at the macroscale. This means that material removal is more sensitive to contact pressure at the macroscale than the nanoscale. In this study, the effect of slide velocity on material removal is not considered because the sliding velocity has been set to the same order of magnitude for both nano- and macro-tribology experiments. Therefore, the difference in material removal capability at the nanoscale and macroscale can be due to different contact pressures. As discussed above, due to the very low real contact stress (lower than the stress that plastic deformation occurs), material removal of PL glass at the nanoscale is dominated by mechanochemical reactions, where the mechanical interaction is very weak. However, due to the multi-asperity contact at the macroscale, the real contact stress for each asperity is much higher than at the nanoscale. Although mechanochemical reactions also play a critical role in the material removal process, the high local contact-stress greatly accelerates mechanical material removal. Owing to the combined action of mechanochemical reaction and mechanical interaction, the material removal growth-ratio at unit pressure is higher at the macroscale. In other words, m can be derived more accurately at the macroscale than at the nanoscale.

4 Conclusions

In this study, the nano- and macro-tribological

properties of PL glass following rubbing against a SiO_2 sphere were investigated using an atomic force microscope and a universal reciprocating sliding tribometer, respectively. This was done to obtain additional insight into the tribological properties of PL glass under both dry and humid conditions. The friction of the PL glass/SiO_2 pair indicates opposing trends at the nanoscale and the macroscale. At the nanoscale, the COF in humid air is higher than that in dry air, which is attributed to the capillary effect associated with the absorbed water film at the interface. Because the interfacial friction dominates the friction process in both dry and humid air, the COF is lower at the nanoscale compared to the macroscale. At the macroscale, on the other hand, the COF in humid air is lower than that in dry air, because the water-related mechanochemical wear makes the wear track surface smoother in the humid air. Owing to the multiasperity contact, the friction at each asperity is dominated by ploughing friction, which causes higher COFs than at the nanoscale.

The material removal of PL glass is more severe in humid air than in dry air at both the nanoscale and macroscale, due to that stress-enhanced hydrolysis accelerates the material removal process of the glass. Furthermore, material removal is found to be more sensitive to contact pressure at the macroscale than at the nanoscale because stronger mechanical interaction occurs in material removal at the macroscale with the multiasperity contact mode. At the macroscale, the material removal process is more sensitive to contact pressure in humid air than in dry air. Because almost all mechanical energy is used to remove material in humid air, whereas most mechanical energy is used to produce cracks in the PL glass in dry air.

Acknowledgements

The authors are grateful for financial support from the National Natural Science Foundation of China (Nos. 51975492 and 51575462), the Scientific Research Fund of Sichuan Provincial Education Department, China (18ZA0504), the Research Fund Supported by Sichuan Science and Technology Program (2018JY0245), the Research Foundation of Southwest University of Science and Technology (18zx7162), the Tribology Science Fund of State Key Laboratory of Tribology (SKLTKF19B15), and the Project National United Engineering Laboratory for Advanced Bearing Tribology, Henan University of Science and Technology (201910).

Electronic Supplementary Material: Supplementary material is available in the online version of this article at https://doi.org/10.1007/s40544-020-0411-2.

References

[1] Campbell J H, Suratwala T I. Nd-doped phosphate glasses for high-energy/high-peak-power lasers. *J Non-Cryst Solids* **263–264**: 318–341 (2000)

[2] Moses E I. Advances in inertial confinement fusion at the national ignition facility (NIF). *Fusion Eng Des* **85**(7–9): 983–986 (2010)

[3] Campbell J H, Hawley-Fedder R A, Stolz C J, Menapace J A, Borden M R, Whitman P K, Yu J, Runkel M J, Riley M O, Feit M D, et al. NIF optical materials and fabrication technologies: An overview. In *Proceedings of SPIE-The International Society for Optical Engineering*, California, USA, 2004: 84–101.

[4] Suratwala T, Feit M, Steele W, Wong L, Shen N, Dylla-Spears R, Desjardin R, Mason D, Geraghty P, Miller P,

et al. Microscopic removal function and the relationship between slurry particle size distribution and workpiece roughness during pad polishing. *J Am Ceram Soc* **97**(1): 81–91 (2014)

[5] Liu E, Blanpain B, Celis J P, Roos J R. Comparative study between macrotribology and nanotribology. *J Appl Phys* **84**(9): 4859–4865 (1998)

[6] Czichos H. Tribology and its many facets: From macroscopic to microscopic and nano-scale phenomena. *Meccanica* **36**(6): 605–615 (2001)

[7] Broitman E. The nature of the frictional force at the macro-, micro-, and nano-scales. *Friction* **2**(1): 40–46 (2014)

[8] Kumar A, Bhushan B. Nanomechanical, nanotribological and macrotribological characterization of hard coatings and surface treatment of H-13 steel. *Tribol Int* **81**: 149–158 (2015)

[9] Yu J X, Qian L M, Yu B J, Zhou Z R. Effect of surface hydrophilicity on the nanofretting behavior of Si(100) in atmosphere and vacuum. *J Appl Phys* **108**(3): 034314 (2010)

[10] Chen L, He H T, Wang X D, Kim S H, Qian L M. Tribology of Si/SiO_2 in humid air: Transition from severe chemical wear to wearless behavior at nanoscale. *Langmuir* **31**(1): 149–156 (2015)

[11] Wang X D, Yu J X, Chen L, Qian L M, Zhou Z R. Effects of water and oxygen on the tribochemical wear of monocrystalline Si(100) against SiO_2 sphere by simulating the contact conditions in MEMS. *Wear* **271** (9–10): 1681–1688 (2011)

[12] Zum Gahr K H, Blattner R, Hwang D H, Pöhlmann K. Micro- and macro-tribological properties of SiC ceramics in sliding contact. *Wear* **250**(1–12): 299–310 (2001)

[13] Qi H M, Hu C, Zhang G, Yu J X, Zhang Y F, He H T. Comparative study of tribological properties of carbon fibers and aramid particles reinforced polyimide composites under dry and sea water lubricated conditions. *Wear* **436–437**: 203001 (2019)

[14] Qiao Q, He H T, Yu J X. Evolution of HF etching rate of borosilicate glass by friction-induced damages. *Appl Surf Sci* **512**: 144789 (2020)

[15] Sun Y X, Song C F, Liu Z L, Li J W, Wang L, Sun C, Zhang Y Z. Tribological and conductive behavior of Cu/Cu rolling current-carrying pairs in a water environment. *Tribol Int* **143**: 106055 (2020)

[16] Sun Y X, Song C F, Liu Z L, Li J W, Sun Y M, Shangguan B, Zhang Y Z. Effect of relative humidity on the tribological/conductive properties of Cu/Cu rolling contact pairs. *Wear* **436–437**: 203023 (2019)

[17] Ye J H, Yu J X, He H T, Zhang Y F. Effect of water on wear of phosphate laser glass and BK7 glass. *Wear* **376–377**: 393–402 (2017)

[18] He H T, Yang L, Yu J X, Zhang Y F, Qi H M. Velocity-dependent wear behavior of phosphate laser glass. *Ceram Int* **45**(16): 19777–19783 (2019)

[19] Yu J X, He H T, Zhang Y F, Hu H L. Nanoscale mechanochemical wear of phosphate laser glass against a CeO_2 particle in humid air. *Appl Surf Sci* **392**: 523–530 (2017)

[20] Fu J C, He H T, Yuan W F, Zhang Y F, Yu J X. Towards a deeper understanding of nanoscratch-induced deformation in an optical glass. *Appl Phys Lett* **113**(3): 031606 (2018)

[21] Yu J X, He H T, Jian Q Y, Zhang W L, Zhang Y F, Yuan W F. Tribochemical wear of phosphate laser glass against silica ball in water. *Tribol Int* **104**: 10–18 (2016)

[22] Etter S, Despetis F, Etienne P. Sub-critical crack growth in some phosphate glasses. *J Non-Cryst Solids* **354**(2–9): 580–586 (2008)

[23] Bunker B C, Arnold G W, Wilder J A. Phosphate glass dissolution in aqueous solutions. *J Non-Cryst Solids* **64**(3): 291–316 (1984)

[24] Bradley L C, Dilworth Z R, Barnette A L, Hsiao E, Barthel A J, Pantano C G, Kim S H. Hydronium ions in soda-lime silicate glass surfaces. *J Am Ceram Soc* **96**(2): 458–463 (2013)

[25] He H T, Qian L M, Pantano C G, Kim S H. Mechanochemical wear of soda lime silica glass in humid environments. *J Am Ceram Soc* **97**(7): 2061–2068 (2014)

[26] Yu J X, Jian Q Y, Yuan W F, Gu B, Ji F, Huang W. Further damage induced by water in micro-indentations in phosphate laser glass. *Appl Surf Sci* **292**: 267–277 (2014)

[27] Brow R K, Click C A, Alam T M. Modifier coordination and phosphate glass networks. *J Non-Cryst Solids* **274**(1-3): 9–16 (2000)

[28] Varenberg M, Etsion I, Halperin G. An improved wedge calibration method for lateral force in atomic force microscopy. *Rev Sci Instrum* **74**(7): 3362–3367 (2003)

[29] Bowden F P, Tabor D. *The Friction and Lubrication of Solids*. London (UK): Oxford University Press, 1958.

[30] Wang Y R, He H T, Yu J X, Zhang Y F, Hu H L. Effect of absorbed water on the adhesion, friction, and wear of phosphate laser glass at nanoscale. *J Am Ceram Soc* **100**(11): 5075–5085 (2017)

[31] Yu J X, Hu H L, Jia F, Yuan W F, Zang H B, Cai Y, Ji F. Quantitative investigation on single-asperity friction and wear of phosphate laser glass against a spherical AFM diamond tip. *Tribol Int* **81**: 43–52 (2015)

[32] Johnson K L. *Contact Mechanics*. Cambridge (UK): Cambridge University Press, 1987.

[33] Xiao X D, Qian L M. Investigation of humidity-dependent capillary force. *Langmuir* **16**(21): 8153–8158 (2000)

[34] He H T, Yu J X, Ye J H, Zhang Y F. On the effect of

tribo-corrosion on reciprocating scratch behaviors of phosphate laser glass. *Int J Appl Glass Sci* **9**(3): 352–363 (2018)

[35] Socrates G. *Infrared and Raman Characteristic Group Frequencies*. Chichester (UK): Wiley, 2001.

[36] Thomas R. Determination of water contents of granite melt inclusions by confocal laser Raman microprobe spectroscopy. *Am Mineral* **85**(5–6): 868–872 (2000)

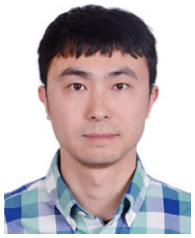

Jiaxin YU. He received his B.S. degree and Ph.D. degree from Southwest Jiaotong University in 2005 and 2011, respectively. From 2015 to 2016, he worked as a research assistant at Yale University in the USA. He is now working as the deputy director of Key Laboratory of Testing Technology for Manufacturing Process in the Ministry of Education, Southwest University of Science and Technology. He is a candidate for academic and technical leaders in Sichuan Province. His current research interests include nanotribology, ultraprecision machining, surface, and interface technology, and tribology of metal-based composite coatings. He has published more than 50 papers in professional journals. As a group leader, he has undertaken more than 20 research projects.

Huimin QI. She received her Ph.D. degree from Lanzhou Institute of Chemical Physics, the Chinese Academy of Sciences, in 2018. She is now working as an associate professor and a master student supervisor in Key Laboratory of Testing Technology for Manufacturing Process in the Ministry of Education, Southwest University of Science and Technology. She interests in the tribology of self-lubricating polymer composites and the frictional interface properties. She has published nearly 20 papers in professional journals.